

Quality Control in Injection Molding based on Norm-optimal Iterative Learning Cavity Pressure Control

Sebastian Stemmler* Marko Vukovic* Muzaffer Ay*
Julian Heinisch** Yannik Lockner** Dirk Abel*
Christian Hopmann**

* *Institute of Automatic Control, RWTH Aachen University, Germany,
52062 Aachen (e-mail: S.Stemmler@irt.rwth-aachen.de)*

** *Institute for Plastics Processing at RWTH Aachen University, 52062
Aachen*

Abstract: Plastic injection molding is characterized by high design flexibility of the manufactured parts. Consequently, it is one of the most important processes for mass production of plastic parts. The setup of the manufacturing process is very complex due to numerous impact factors. In addition, material fluctuations or changing ambient conditions require the adaption of the setup during manufacturing to guarantee a constant product quality.

In order to reduce the setup effort and to control the quality, the concept of model-based self-optimization is applied to injection molding. Therefore, a model-based Norm-Optimal Iterative Learning Controller (NOILC) is used to track a desired reference for the cavity pressure during the entire cycle. This reference is determined by the so-called pvT-optimization which considers the cooling behavior of the melt within the cavity. It is shown by experiments that the cavity pressure can be controlled with high accuracy using the presented NOILC. Furthermore, the accuracy of the quality, especially the part weight is improved by combining the NOILC with an additional pvT-optimization.

Keywords: Lifted System Notation, Iterative Learning Control, Extended Kalman Filter, Quality Control, Injection Molding, pvT-Optimization, Manufacturing

1. INTRODUCTION

Injection molding of thermoplastics is one of the most important processes for manufacturing of plastic parts. The parts are manufactured by injection molding machines which in a simplified way consist of a plasticizing unit and a mold (Fig 1). The task of the plasticizing unit (5) is to melt the thermoplastic granulate, to dose it and inject it into the cavity (2) of the mold (1). Consequently, the shape depends on the geometry of the cavity. Therefore, the mold has to be designed and manufactured individually for each part.

Plastic injection molding is a discontinuous manufacturing process, since the process steps are repeated cyclical. At the beginning of each cycle, the granulate is fed via the hopper (6) into the plasticizing unit by a rotation of the screw (4), which in this case is actuated by a servo-electric drive (7). As a result of the friction between plastics, screw and the wall of the barrel the granulate is plasticized. At the same time the melt temperature is controlled by heating elements which are mounted on the outer wall of the plasticizing cylinder. During dosing, the screw performs a rotational movement superposed by a translational rearward movement, filling and enlarging the screw antechamber (3) until the desired melt injection volume is reached. The plastic melt is then injected into the cavity by a translational screw movement. Once the melt enters the tempered mold, it is cooled down. This

results in shrinkage of the melt during the solidification process which is compensated in the so-called packing phase by a mass flow from the screw antechamber into the cavity until the gate is solidified. The melt within the cavity cools further down until the part is ejected and a new cycle begins.

Injection molding machines have numerous sensors already integrated and thus have a high potential for automation. In order to increase the level of automation e. g. Thombsen et al. (2018); Djurdjanovic et al. (2018) propose the establishment of both process and quality control loops. Therefore, further sensors have to be integrated in the process to monitor e. g. temperature and pressure within the cavity. This enables the observation of these values and consequently the development of higher control loops. Due to the nonlinear material behavior classical controllers (e. g. PID-controllers) are not suitable for the application in such control loops, see e. g. Agrawal et al. (1987). For this reason, the parameters of the PID-controllers are adapted to the current system state, as done by Gao et al. (1994); Kazmer and Barkan (1997). However, these approaches have to be parameterized for each mold which is time-consuming. In order to simplify the parameterization, numerous model-based controllers are researched. Here different controlled variables were examined in the related literature, which are applied for the screw velocity, the injection velocity, the drive pressure or the drive force, the cavity pressure as well as the melt

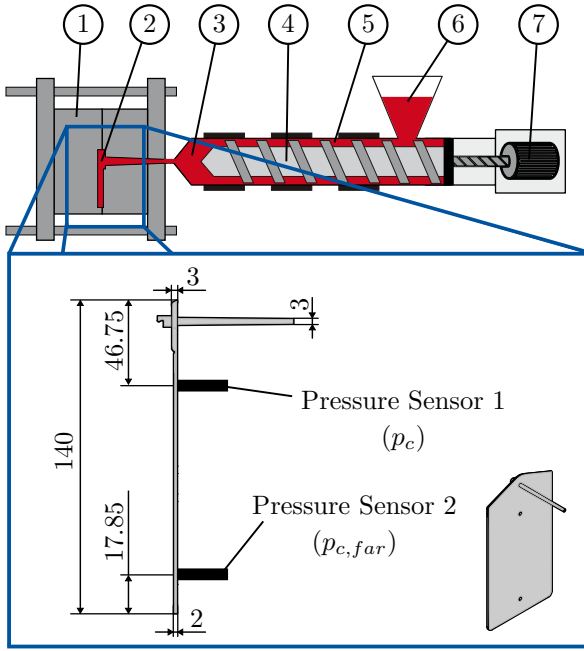


Fig. 1. Schematic structure of a plastic injection molding machine with the geometry of the manufactured plate and the positions of the pressure sensors.

temperature. See for example Dubay et al. (2014); Lindert et al. (2014); Li et al. (2010); Michaeli and Schreiber (2009); Froehlich et al. (2019).

First approaches, e. g. Chen et al. (2008b), use quality models in order to control the part quality. However, since no physical correlation exists between the machine values and the quality values, empirical models are used. Furthermore, an adaptive, iterative learning controller is described by Chen et al. (2008a), which is based on a repetitive parameter estimation. In addition, Schiffers (2009); Tellaeché and Arana (2013) adapt the machine settings with respect to an empirical quality model. In the cited literature all system models are based on empirical data. Thus, the models and in consequence the derived controllers are only valid for a known and trained combination of machine, mold and material.

In prior work two different model-based predictive controller approaches as well as a Norm-Optimal Iterative Learning Controller (NOILC) were researched for cavity pressure control which are described in Reiter et al. (2014); Hopmann et al. (2017); Stemmler et al. (2019). In this contribution the concept of model-based self-optimization, which is described in Brecher (2017); Thombansen et al. (2018) is applied and validated in injection molding. It enables part Therefore, the proposed NOILC is used as a process controller which tracks an optimal cavity pressure reference during the entire cycle. In contrast to prior work a physically-motivated model is explicitly used within the NOILC, which increases the tracking performance for cavity pressure. Furthermore, this NOILC enables cross-phase cavity pressure control. The cavity pressure reference is determined by the pvT-optimization, which considers a material model in order to describe the specific volume and in consequence the weight with respect to process values. The proposed control architecture is depicted in Fig. 2, which is also reflected in the following.

2. PROCESS MODEL

In order to develop the model-based NOILC, the process has to be modeled. For this purpose, the injection molding process is described in accordance to Stemmler et al. (2019) by two pressure vessels which are connected by a flow channel (Fig 3). While the first pressure vessel describes the cavity (2) with a constant geometric volume, the second pressure vessel represents the plasification unit (3). Its geometric volume depends on the position of the screw (4) which is actuated by a servo-electric drive (7) whose velocity is already controlled by machine-oriented control loops. Based on this assumptions, the state vector

$$\mathbf{X} = (X_1 \ X_2 \ X_3 \ X_4 \ X_5)^T := (x \ v \ \dot{v} \ p_s \ p_c)^T \quad (1)$$

is introduced. Both the position x and the velocity v of the screw are given in terms of screw antechamber's volume:

$$v = v_s A_s = \frac{dx}{dt} = A_s \frac{dx_s}{dt}, \quad (2)$$

with the screw area A_s , the screw position x_s and the screw velocity v_s regarding Fig. 3. Furthermore, the state vector (1) is defined by the acceleration \dot{v} , the screw pressure p_s and the cavity pressure p_c . The screw pressure p_s describes the pressure in front of the screw which is approximated by the applied force of the drive. The cavity pressure p_c is measured by a pressure sensor within the cavity (Fig. 1). According to Stemmler et al. (2019), the state equations

$$\dot{\mathbf{X}} = \begin{pmatrix} X_2 \\ X_3 \\ -2D\omega_0 X_3 - \omega_0^2 X_2 + K_D \omega_0^2 U_v \\ \frac{\beta_s}{X_1} \left(-X_2 - \frac{\pi R^4}{8L\eta} (X_4 - X_5) \right) \\ f_5(\mathbf{X}) \end{pmatrix} \quad (3)$$

are established. Thereby, the parameters D , w_0 and K_D parameterize a second order system which is assumed to describe the dynamic behavior of the drive. The control voltage U_v is the input of the system which corresponds to a desired screw velocity. Since the plasticizing unit is assumed as a pressure vessel, its dynamic behavior is described by the mass-continuity equation and thus depends on the bulk modulus β_s . Furthermore, the screw pressure p_s depends on the mass flow \dot{m}_n through the gate which is characterized by its radius R , length L , the dynamic viscosity η and the pressure gradient. The dynamic viscosity η is identified empirically and approximated by

$$\eta(t) := \begin{cases} \eta_0 & \text{for } p_{c, far} \leq p_{sw} \\ \eta_0 + \Delta\eta (t - t_{sw}) & \text{for } p_{c, far} > p_{sw} \end{cases} \quad (4)$$

with the viscosity η_0 during the injection phase and the slope $\Delta\eta$. Thus, nonlinearities of the process can be approximated and lumped into the viscosity. As its behavior depends on the filling level of the cavity the pressure $p_{c, far}$ is measured at the end of the flow path (Fig. 1). If the pressure $p_{c, far}$ is greater than the threshold pressure value p_{sw} the cavity is assumed to be completely filled and the time t_{sw} is determined. Similarly, the sixth state equation of (3) is distinguished:

$$f_5(\mathbf{X}) := \begin{cases} -\omega_2 X_5 + K_2 p_s^* & \text{for } p_{c, far} \leq p_{sw}, \\ \frac{\beta_c}{V_0} \frac{\pi R^4}{8L\eta} (X_4 - X_5) & \text{for } p_{c, far} > p_{sw}. \end{cases} \quad (5)$$

According to Stemmler et al. (2019), the cavity pressure is approximated by a first order system with time delay

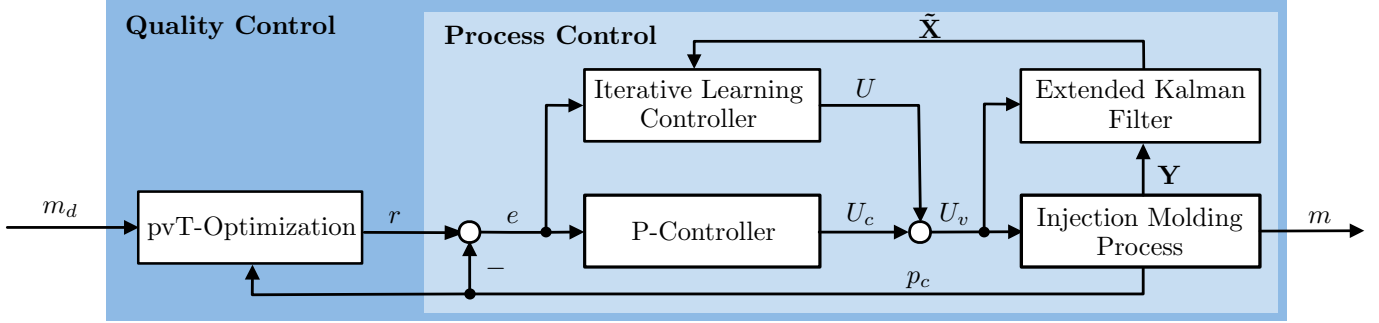


Fig. 2. Control architecture of the proposed quality control based on the pvT-optimization and a process control scheme which consists of an iterative learning controller and an extended kalman filter.

$T_{d,c}$ during the injection phase. The screw pressure p_s is defined as the input of this first order system. The state equation is parameterized by the parameters K_2 and w_2 . To account for the time delay of the first order system the screw pressure is delayed by

$$p_s^*(t) := \begin{cases} X_4(t - T_{d,c}) & \text{for } t > T_{d,c}, \\ 0 & \text{otherwise.} \end{cases} \quad (6)$$

When the cavity is fully filled, the behavior of the cavity pressure vessel is described by the mass continuity equation, too. Accordingly, its dynamics depend on the bulk modulus β_c of the melt, the geometric volume V_0 of the cavity and the mass flow \dot{m}_n through the channel (Fig. 3).

3. PVT-OPTIMIZATION

As discussed in Hopmann et al. (2016) the quality depends significantly on the cavity pressure during the cooling phase. Due to the melt cooling, the specific volume decreases and thus volume shrinkage occurs. This can be described by the pressure-volume-temperature diagram (pvT-diagram) which is depicted for a semi-crystalline thermoplastic in Fig. 4. In this contribution the 7-coefficient approach

$$v_c(p_c, T_c) := \begin{cases} \frac{K_1^s}{p_c + K_4^s} + \frac{K_2^s T_c}{p_c + K_3^s} + K^* & \text{for } T_c < T_f, \\ \frac{K_1^f}{p_c + K_4^f} + \frac{K_2^f T_c}{p_c + K_3^f} & \text{otherwise,} \end{cases} \quad (7)$$

$$K^*(p_c, T_c) := K_5^s e^{K_6^s T_c - K_7^s p_c}. \quad (8)$$

is used, which was proposed by Schmidt (1986). As a result, the melt's specific volume v_c within in the cavity can be derived from the cavity pressure p_c and the melt temperature T_c . The transit temperature T_f , at which the melt changes from the solid state to the liquid state is given by

$$T_f(p_c) := K_8 + K_9 p_c. \quad (9)$$

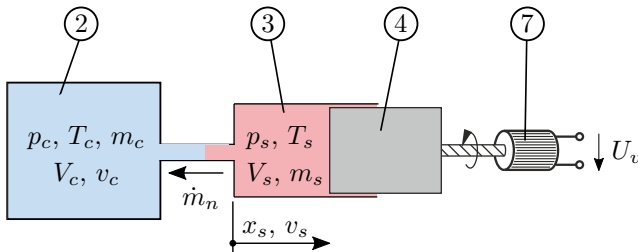


Fig. 3. Schematic sketch of the simplified process model. Its elements are numbered in analogy to Fig. 1.

The material-dependent parameters $K_1^s, K_2^s, K_3^s, K_4^s, K_5^s, K_6^s, K_7^s, K_1^f, K_2^f, K_3^f, K_4^f, K_8$ and K_9 are determined empirically and given in Tab. 1 for polypropylene of type PP579S (Sabic Germany GmbH & Co. KG, Dusseldorf, Germany), which is used in this contribution.

Assuming a homogeneous distribution of both the pressure and temperature within the cavity an optimal pressure trajectory can be determined in accordance to Hopmann et al. (2016, 2017) which is depicted in Fig. 4 in red. Accordingly, the melt should be isothermally injected into the cavity (A to B) until the cavity is fully filled. For this purpose, the melt must be injected as quickly as possible. Afterwards, the melt cools down and thus the specific volume decreases. The shrinkage is compensated during the isobaric pressure holding phase (B to C) by an additional mass flow into the cavity. Subsequently, the melt cools down isochorously until the gate is fully frozen (C to D). As a result, no further melt flows into the cavity.

If point D can be reproduced exactly in each manufacturing cycle, the volume shrinkage and thus the part weight is identical for all manufacturing cycles. Consequently, the desired part weight m_d has to be defined in a first step.

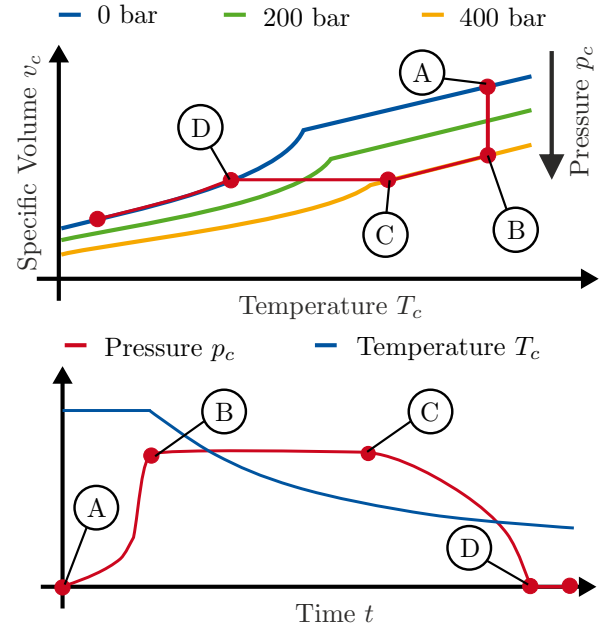


Fig. 4. pvT-diagram of semi-crystalline thermoplastic (top) with the optimal pressure trajectory (red line) and the corresponding melt temperature T_c within the cavity (bottom).

Table 1. Material parameters of polypropylen (PP579S).

Symbol	Value	Symbol	Value
K_1^f	21 406.79 s ⁻²	K_1^s	28 683.12 s ⁻²
K_2^f	1.82 °C ⁻¹ s ⁻²	K_2^s	1.04 °C ⁻¹ s ⁻²
K_3^f	1695.67 bar	K_3^s	1261.56 bar
K_4^f	17 977.94 bar	K_4^s	25 397.45 bar
K_8	122.33 °C	K_5^s	7.41 · 10 ⁻⁶ cm ³ g ⁻¹
K_9	2.04 · 10 ⁻² °C bar ⁻¹	K_6^s	7.72 · 10 ⁻² °C ⁻¹
		K_7^s	1.85 · 10 ⁻³ bar ⁻¹

Then, the required specific volume v_d has to be determined with respect to the geometric volume V_0 of the cavity according to

$$v_d := \frac{V_0}{m_d} \quad (10)$$

which is given for an ambient temperature T_0 and pressure p_0 , respectively. Since the melt is solidified below the transition temperature $T_f(p_c)$ no further melt flows into the cavity for $T_c < T_f(p_c)$. However, the melt close to the pressure sensor 1 (Fig. 1) freezes before the gate. For this reason, an offset has to be considered and therefore the specific volume $v_c(p_0, T_D)$ is defined in point D for temperature T_D . Afterwards, the optimization problem

$$\min_r \|v_c(p_0, T_D) - v_c(r, T_c)\| \quad (11)$$

is solved in each time instance in order to determine the optimal cavity pressure reference r . Moreover, the constraint $r < p_{c,max}$ is considered in order to limit the maximum cavity pressure during the isobaric pressure holding phase. Furthermore, the melt temperature T_c as well as its prediction is required for the mentioned optimization problem (11). For this reason, the temperature T_c is approximated by the cooling equation

$$T_c(t) := T_m + \frac{8}{\pi^2} (T_s - T_m) e^{-\alpha \left(\frac{\pi}{d}\right)^2 (t - t_{sw})} \quad (12)$$

for $t > t_{sw}$. Otherwise it is assumed as constant with $T_c(t = t_{sw})$ in order to approximate the isothermal injection phase. This approach is discussed in Bongart (1982) and depends on the mold temperature T_m , the temperature T_s and the thermal conductivity α of the melt as well as the part thickness d at the sensor position. The optimization problem (11) is solved by the bisection method which is described in Quarteroni et al. (2007).

4. NORM-OPTIMAL ITERATIVE LEARNING CAVITY PRESSURE CONTROL

In order to track the reference r a NOILC is applied which uses a piece-wise linearized model around the trajectories of the previous cycle. For this, the state vector \mathbf{x} has to be estimated by an Extended Kalman Filter (EKF) as not all of its states can be measured. The EKF also linearizes the process model in each time instance. For this reason, the piece-wise linearization is first introduced. Then the EKF as well as the NOILC are presented.

4.1 Piece-wise Linearization

In accordance to Stemmler et al. (2019), the state equations (3) are linearized in each time instance in order to determine the time-variant, linear state-space model

$$\dot{\mathbf{x}} = \mathbf{A}_t \mathbf{x} + \mathbf{b}_t u_v \quad (13)$$

$$\mathbf{y} = \mathbf{C}_t \mathbf{x} \quad (14)$$

with the time-variant system matrices \mathbf{A}_t , \mathbf{b}_t , \mathbf{C}_t and the relative values

$$\mathbf{x} := \mathbf{X} - \mathbf{X}_{op}, \quad u_v := U_v - U_{op}, \quad \mathbf{y} := \mathbf{Y} - \mathbf{Y}_{op}. \quad (15)$$

The operation points $(\mathbf{X}_{op}, U_{v,op}, \mathbf{Y}_{op})$ are determined by the values $(\mathbf{X}, U_v, \mathbf{Y})$ of the previous cycle. The output equation (14) is different for the EKF and the NOILC and thus is discussed later. The mentioned time-variant state-space model is then discretized with the sample time T in each time instance in order to get the time discrete state-space model

$$\begin{aligned} \mathbf{x}(k+1) &= \mathbf{A}_k \mathbf{x}(k) + \mathbf{b}_k u_v(k) \\ \mathbf{y}(k) &= \mathbf{C}_k \mathbf{x}(k) \end{aligned} \quad (16)$$

with the time-variant system matrices \mathbf{A}_k , \mathbf{b}_k and \mathbf{c}^T .

4.2 Extended Kalman Filter

In the presented case, only the position x as well as the velocity v of the screw, the pressure p_s at the tip of the screw and the cavity pressure p_c can be measured. Consequently, the output vector is defined by

$$\mathbf{Y} = \mathbf{C}_k \mathbf{X} = (X_1 \ X_2 \ X_4 \ X_5)^T. \quad (17)$$

Since the complete state vector \mathbf{X} is required for the piece-wise linearization, the state vector $\tilde{\mathbf{X}}$ is estimated by an EKF and then used as the operation point in (15).

In accordance to Grewal and Adreus (2008), the EKF is divided into a correction step and a prediction step. The correction step is defined by

$$\mathbf{K}(k) = \hat{\mathbf{P}}(k) \mathbf{A}_k^T \left(\mathbf{C}_k \hat{\mathbf{P}}(k) \mathbf{C}_k^T + \mathbf{R} \right)^{-1} \quad (18)$$

$$\tilde{\mathbf{X}}(k) = \hat{\mathbf{X}}(k) + \mathbf{K}(k) \left(\mathbf{Y}(k) - \mathbf{C}_k \hat{\mathbf{X}}(k) \right) \quad (19)$$

$$\tilde{\mathbf{P}}(k) = (\mathbf{I} - \mathbf{K}(k) \mathbf{C}_k) \hat{\mathbf{P}}(k) \quad (20)$$

with the kalman gain \mathbf{K} , the corrected covariance matrix $\tilde{\mathbf{P}}$ and the identity matrix \mathbf{I} . The predicted state vector $\hat{\mathbf{X}}$ and the corresponding predicted covariance matrix $\hat{\mathbf{P}}$ are determined during the prediction step of the EKF:

$$\hat{\mathbf{X}}(k+1) = \tilde{\mathbf{X}}(k) + T \varphi \left(\mathbf{f} \left(\tilde{\mathbf{X}}(k), U_v(k) \right) \right) \quad (21)$$

$$\hat{\mathbf{P}}(k+1) = \mathbf{A}_k \tilde{\mathbf{P}}(k) \mathbf{A}_k^T + \mathbf{Q} \quad (22)$$

with the sample time T of the EKF. The positive definite covariance matrices

$$\mathbf{Q} = \delta \mathbf{I}, \quad \mathbf{R} = \epsilon \mathbf{I} \quad (23)$$

are parameterized by the tuning parameters δ , ϵ with respect to the process noise and the measurement noise, respectively. The calculation of the progress functions φ is realized by the Runge-Kutta-method of fourth order, which is described in Butcher (2008).

4.3 Lifted System Notation

To control the cavity pressure p_c by adapting the control voltage U_v the output equation (14) yields

$$\mathbf{Y} = \mathbf{c}_k \mathbf{X} = (0 \ 0 \ 0 \ 0 \ 1) \mathbf{X}. \quad (24)$$

Furthermore, the cavity pressure p_c is controlled by a P-controller in order to realize a desired transfer behavior

(see Fig. 2). Therefore the closed loop has to be considered in the NOILC by defining

$$U_v = U_c + U = K_p X_5 + U \quad (25)$$

with the output U_c of the P-controller and the output U of the NOILC. Consequently, the time discrete model (16) can be reformulated by

$$\begin{aligned} \mathbf{x}(k+1) &= \tilde{\mathbf{A}}_k \mathbf{x}(k) + \tilde{\mathbf{b}}_k u(k) \\ y(k) &= \tilde{\mathbf{c}}_k \mathbf{x}(k) \end{aligned} \quad (26)$$

with the state matrix $\tilde{\mathbf{A}}_k$, the input matrix $\tilde{\mathbf{b}}_k$ and the measurement matrix $\tilde{\mathbf{c}}_k$ of the controlled system. Based on this model the NOILC can be formulated.

In contrast to most control approaches, the NOILC considers the input sequence \mathbf{u}_j and the output sequence \mathbf{y}_j of the complete cycle j . They are defined by

$$\mathbf{u}_j = (u(1) \ u(2) \ \dots \ u(N_c))^T, \quad (27)$$

$$\mathbf{y}_j = (y(1) \ y(2) \ \dots \ y(N_c))^T, \quad (28)$$

with the number N_c of time steps within one cycle. Taking this definition into account, the transfer behavior of the controlled system is described by the lifted system notation

$$\mathbf{y}_j = \mathbf{G} \mathbf{u}_j + \mathbf{y}^* \quad (29)$$

with the transfer matrix \mathbf{G} and the initial output vector \mathbf{y}^* . Here, the initial output vector \mathbf{y}^* describes the influence of the initial system states $\mathbf{x}(0)$ to the output sequence \mathbf{y}_j . Referring to Hakvoort et al. (2007) the transfer matrix \mathbf{G} and the initial output vector \mathbf{y}^* are defined by

$$\mathbf{G} := \begin{bmatrix} 0 & 0 & \dots & 0 \\ \tilde{\mathbf{c}}_2 \tilde{\mathbf{b}}_1 & 0 & \dots & 0 \\ \tilde{\mathbf{c}}_3 \tilde{\mathbf{A}}_2 \tilde{\mathbf{b}}_1 & \tilde{\mathbf{c}}_3 \tilde{\mathbf{b}}_2 & \dots & 0 \\ \tilde{\mathbf{c}}_4 \tilde{\mathbf{A}}_3 \tilde{\mathbf{A}}_2 \tilde{\mathbf{b}}_1 & \tilde{\mathbf{c}}_4 \tilde{\mathbf{A}}_2 \tilde{\mathbf{b}}_2 & \dots & 0 \\ \vdots & \vdots & \ddots & \vdots \\ \tilde{\mathbf{c}}_{N_c} \left(\prod_{i=2}^{N_c-1} \tilde{\mathbf{A}}_i \right) \tilde{\mathbf{b}}_1 & \tilde{\mathbf{c}}_{N_c} \left(\prod_{i=3}^{N_c-1} \tilde{\mathbf{A}}_i \right) \tilde{\mathbf{b}}_2 & \dots & 0 \end{bmatrix}, \quad (30)$$

$$\mathbf{y}^* = \begin{bmatrix} \tilde{\mathbf{c}}_1 \tilde{\mathbf{A}}_0 \\ \tilde{\mathbf{c}}_2 \tilde{\mathbf{A}}_1 \tilde{\mathbf{A}}_0 \\ \tilde{\mathbf{c}}_3 \tilde{\mathbf{A}}_2 \tilde{\mathbf{A}}_1 \tilde{\mathbf{A}}_0 \\ \vdots \\ \tilde{\mathbf{c}}_{N_c} \prod_{i=0}^{N_c-1} \tilde{\mathbf{A}}_i \end{bmatrix} \mathbf{x}(0), \quad (31)$$

which is considered explicitly in the optimization problem of the NOILC.

4.4 Optimization Problem

In accordance to Hopmann et al. (2017) the control law of the NOILC yields

$$\mathbf{u}_{j+1} = \mathbf{u}_j + \gamma \Delta \mathbf{u}_{j+1} \quad (32)$$

Accordingly, the input sequence \mathbf{u}_{j+1} for the next cycle is calculated with respect to the input sequence \mathbf{u}_j of the previous cycle and an optimal control deviation $\Delta \mathbf{u}_{j+1}$ which is weighted by the learning operator γ . The optimal control deviation $\Delta \mathbf{u}_{j+1}$ is determined by an optimization. The computing time of the optimization is influenced significantly by the number of optimization variables. In

order to reduce the number of optimization variables piecewise splines of third order are defined, whose parameters are determined by the optimization. This reduces the number of optimization variables and thus the computation time. Consequently, the optimal control deviation is substituted by

$$\Delta \mathbf{u}_{j+1} = \mathbf{M}_T \mathbf{P}_{j+1} \quad (33)$$

with the parameter vector \mathbf{P}_{j+1} and the transformation matrix \mathbf{M}_T . The parameter vector \mathbf{P}_{j+1} depends on the number of intervals N_I which are defined for the cycle. The parameter vector is defined by

$$\mathbf{P}_{j+1} := (\mathbf{p}_1^T \ \mathbf{p}_2^T \ \mathbf{p}_3^T \ \dots \ \mathbf{p}_{N_I}^T)^T \quad (34)$$

with the parameter vector of the i -th polynomial

$$\mathbf{p}_i := (a_{3,i} \ a_{2,i} \ a_{1,i} \ a_{0,i})^T. \quad (35)$$

and its coefficients $a_{3,i}$, $a_{2,i}$, $a_{1,i}$, $a_{0,i}$. The transformation matrix \mathbf{M}_T is defined by

$$\mathbf{M}_T := \begin{bmatrix} \mathbf{T} & \mathbf{0} & \mathbf{0} & \dots & \mathbf{0} \\ \mathbf{T}_e & \mathbf{T} & \mathbf{0} & \dots & \mathbf{0} \\ \mathbf{T}_e & \mathbf{T}_e & \mathbf{T} & \dots & \mathbf{0} \\ \vdots & \vdots & \vdots & \ddots & \vdots \\ \mathbf{T}_e & \mathbf{T}_e & \mathbf{T}_e & \dots & \mathbf{T} \end{bmatrix}, \quad (36)$$

with the time matrix

$$\mathbf{T} := [\mathbf{t}_I^3 \ \mathbf{t}_I^2 \ \mathbf{t}_I^1 \ \mathbf{t}_I^0]. \quad (37)$$

Its elements are defined for each interval by

$$\mathbf{t}_I := (0 \ T \ 2T \ 3T \ \dots \ N_s T)^T, \quad (38)$$

with the sample time T and the number N_s of time steps within an interval. In order to prevent discontinuity at the interval boundaries, the terminal functional values of each interval must correspond to the initial values of the following interval. For this purpose, the terminal time matrix

$$\mathbf{T}_e := \mathbf{I}_{N_s \times 1} \mathbf{t}_e \quad (39)$$

is defined, with the identity matrix \mathbf{I} and the time vector

$$\mathbf{t}_e := ((N_s T_s)^3 \ (N_s T_s)^2 \ \dots \ (N_s T_s)^1 \ (N_s T_s)^0). \quad (40)$$

In order to track the reference sequence

$$\mathbf{r}_j = (r(1) \ r(2) \ \dots \ r(N_c))^T, \quad (41)$$

which is determined by the pvT-optimization, the tracking error $\hat{\mathbf{e}} := \mathbf{r}_{j+1} - \hat{\mathbf{y}}_{j+1}$ has to be minimized by the optimization. Furthermore, the controller output deviations within a cycle shall be penalized in order to prevent large changes of the controller output. For this reason, the cost function

$J_{j+1}(\Delta \mathbf{u}_{j+1}) = \|\mathbf{r}_{j+1} - \hat{\mathbf{y}}_{j+1}\|_{\mathbf{S}}^2 + \|\mathbf{M}_\delta \Delta \mathbf{u}_{j+1}\|_{\mathbf{T}}^2$ (42) is defined with the positive definite weighting matrices

$$\mathbf{S} = \lambda \mathbf{I}, \quad \mathbf{T} = \kappa \mathbf{I}, \quad (43)$$

which are parameterized by the tuning parameters λ and κ . The matrix \mathbf{M}_δ is defined by

$$\mathbf{M}_\delta := \begin{bmatrix} 1 & 0 & 0 & \dots & 0 & 0 \\ -1 & 1 & 0 & \dots & 0 & 0 \\ 0 & -1 & 1 & \dots & 0 & 0 \\ 0 & 0 & -1 & \dots & 0 & 0 \\ \vdots & \vdots & \vdots & \ddots & \vdots & \vdots \\ 0 & 0 & 0 & \dots & -1 & 1 \end{bmatrix}. \quad (44)$$

in order to determine the controller output changes between two time instances. The predicted output sequence

$$\hat{\mathbf{y}}_{j+1} = \mathbf{y}_j + \mathbf{G} \Delta \mathbf{u}_{j+1} + \mathbf{y}_0. \quad (45)$$

is given by (29) and the output sequence \mathbf{y}_j of the previous cycle j , where \mathbf{G} represents the block impulse response. Substituting (33) in (42) results in the quadratic optimization problem

$$\min_{\mathbf{P}_{j+1}} \mathbf{P}_{j+1}^T \tilde{\mathbf{H}} \mathbf{P}_{j+1} + \tilde{\mathbf{g}}^T \mathbf{P}_{j+1} \quad (46)$$

with the hessian matrix $\tilde{\mathbf{H}}$ and the gradient vector $\tilde{\mathbf{g}}$

$$\tilde{\mathbf{H}} := \mathbf{M}_T^T \mathbf{G}^T \mathbf{S} \mathbf{G} \mathbf{M}_T + \mathbf{M}_\delta \mathbf{T}, \quad (47)$$

$$\tilde{\mathbf{g}} := 2 \mathbf{e}_{j+1}^T \mathbf{S} \mathbf{G} \mathbf{M}_T. \quad (48)$$

The free tracking error \mathbf{e}_{j+1} is defined by

$$\mathbf{e}_{j+1} = \mathbf{r}_{j+1} - \mathbf{y}_j. \quad (49)$$

Furthermore, the controller output is constrained by

$$\mathbf{u}_{min} \leq \mathbf{u}_j + \gamma \mathbf{M}_T \mathbf{P}_{j+1} \leq \mathbf{u}_{max}. \quad (50)$$

have to be considered in order to taking technical limitations into account in the optimization problem. This constraints can be transformed into

$$\begin{bmatrix} \gamma \mathbf{M}_T \mathbf{I} \\ -\gamma \mathbf{M}_T \mathbf{I} \end{bmatrix} \Delta \mathbf{u}_{j+1} \leq \begin{pmatrix} \mathbf{u}_{max} - \mathbf{u}_j \\ -\mathbf{u}_{min} + \mathbf{u}_j \end{pmatrix} \quad (51)$$

and thus be considered explicitly in the optimization problem (46), which is solved by the qpOASES solver, refer to Ferreau et al. (2014).

5. EXPERIMENTAL RESULTS

The derived control structure (see Fig. 2) is applied to a servo-electric injection molding machine of the type “Allrounder 370 A 600-170/170” which is manufactured by Arburg GmbH & Co KG, Lossburg, Germany. Furthermore, a screw with $A_s = 30$ mm and a cavity volume $V_0 = 33.5 \text{ cm}^3$ is used. The controller model is parameterized in accordance to Tab. 2. Process and machine parameters, which are not taken into account in the NOILC, are set in accordance to the manufacturer’s recommendations in order to guarantee real production conditions. In particular, this applies to the melt temperature $T_s = 220^\circ\text{C}$ in the plastification unit and the supply temperature of the mold control which corresponds in good approximation to the mold temperature $T_m = 30^\circ\text{C}$. For further informations see Stemmler et al. (2019).

For safety reasons, the injection process is started with a constant injection velocity. When a screw pressure of $p_s = 10$ bar is reached the controller is activated. The controller is deactivated after the screw pressure falls below 50 bar. To prevent high velocities of the screw, the control voltage is constrained to

$$-0.5 \text{ V} \leq U_v \leq 0.5 \text{ V}. \quad (52)$$

Furthermore, the NOILC is parameterized by $\lambda = 1$, $\kappa = 10^4$ and $\gamma = 0.5$. The sampling time is $T_s = 8$ ms and the number of sampling steps amounts to $N_c = 1000$ are used, which correspond to a cycle time of 8 s. The length of the spline intervals is set to $N_s = 25$.

The experimental results are shown in Fig. 5 and Fig. 6, respectively. During the first cycle, only the P-controller is active in order to generate initial data for the NOILC. The P-controller is parameterized conservatively in order to prevent overshooting or oscillations of the cavity pressure. In consequence, the cavity pressure reacts slow to tracking errors. In addition, the reactive behavior of the P-controller can be seen at the end of the cycle. From the second cycle onwards, the NOILC is active and optimizes

Table 2. Model parameterization for EKF and NOILC.

Symbol	Value	Symbol	Value
L	8.0 cm	D	0.79
R	0.2 cm	ω_0	133 s ⁻¹
η_0	60/10 ⁵ kg m ⁻¹ s ⁻¹	ω_2	4.9 × 10 ⁻¹⁰ s ⁻¹
$\Delta\eta$	360/10 ⁵ kg m ⁻¹ s ⁻²	$T_{d,c}$	0.94 s
K_D	23.4 cm ³ (s V) ⁻¹	β_s	8662 bar
K_2	0.352 s ⁻¹	β_c	8662 bar
K_p	-0.005 V bar ⁻¹	p_{sw}	10 bar
α	7.03 · 10 ⁻² s mm ⁻²	d	2 mm

the manipulated variable so that the measured cavity pressure converges continuously to the the reference curve. After 10 cycles the reference r , which is determined by the pvT-optimization, is almost tracked perfectly.

After 15 cycles the tempering system of the mold is switched off. As a consequence, the mold temperature T_m increases and thus the cooling behavior of the melt changes. This is considered in terms of the pvT-optimization. Therefore, the determined optimal cavity pressure reference is adapted by the pvT-optimization. For this reason, the final ramp in the reference r is shifted. Nevertheless, the NOILC shows good tracking performance steering the cavity pressure to the new reference. Only in the transition phase between the isobaric pressure holding phase and the ramp a tracking error occurs, because the NOILC cannot follow the continuous change in the reference r fast enough.

In general, it can be stated that the NOILC shows a very small tracking error after a few cycles. This high learning speed results from the learning factor in combination with the accuracy of the used process model. It describes the general behavior of the process, which is consequently considered for prediction within in the controller. If the model shows greater uncertainties, the learning factor should be reduced. However, this also decreases the learning speed of the NOILC.

In order to validate the quality control loop, experiments are carried out with a constant reference $r = 300$ bar as well as with the pvT-optimization (Fig. 7). As mentioned before, the tempering system of the mold is deactivated after 15 cycles and thus the mold temperature increases. After 30 cycles, the tempering system is switched on and thus the mold cools down again. At the beginning of each manufacturing cycle, the mold temperature is measured. The part weight m is measured at the end of each cycle using the precision weighting machine “LA 620S-OCE”, Sartorius AG Germany.

The desired weight is set to 29.1 g. Without the pvT-optimization, the minimum weight is 27.25 g and the maximum weight is 28.11 g. Accordingly, an absolute tolerance of 0.86 g results. When deriving the pressure reference from the pvT-optimization, a minimum weight of 27.93 g and a maximum weight of 28.41 g is achieved. This corresponds to an absolute tolerance of 0.48 g, which approximately halves the weight interval in comparison to the parts manufactured with non-optimized reference values. The main reason for the weight deviations refers to the single measuring point within the cavity. In reality, the melt cools down inhomogenously which is not considered in the mentioned approach. Furthermore, the pvT-diagram is determined under laboratory conditions, so that the pvT diagram does

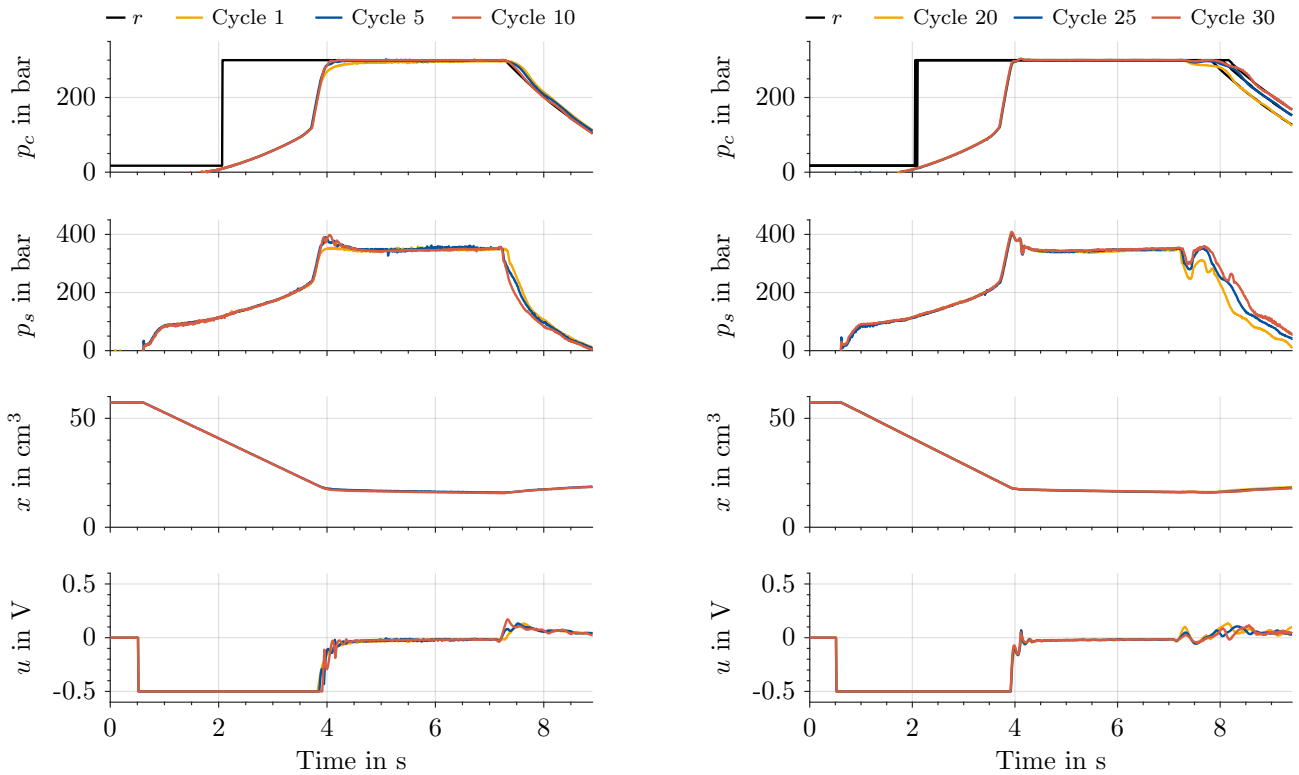


Fig. 5. Experimental results of the process controller for a constant (left) and a varying mold temperature (right). The reference r represents the trajectory which is determined by the pvT-optimization.

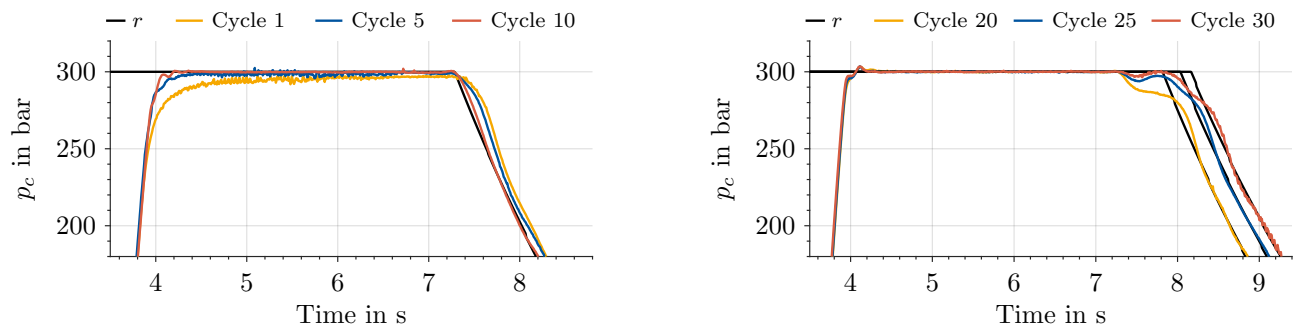


Fig. 6. Detailed view of the cavity pressure from Fig. 5 for a constant (left) and a varying mold temperature (right).

not exactly represent the real process conditions. However, the weight accuracy is more important for production than the absolute desired weight.

6. CONCLUSION

The presented contribution describes an approach for quality control, especially the control of the part weight, in plastic injection molding. The aim was to increase the accuracy of the part weight by combining a model-based cavity pressure controller with the pvT-optimization. For this purpose, sensors are used within the cavity which enable the consideration of process behavior in a model-based, norm-optimal iterative learning cavity pressure controller. This allows a better tracking of any cavity pressure trajectory. Also, the part weight spectrum can be halved by application of the pvT-optimization in comparison to experiments with an constant cavity pressure reference. In further work, the practicability of the presented concept for different molds and materials have to be researched.

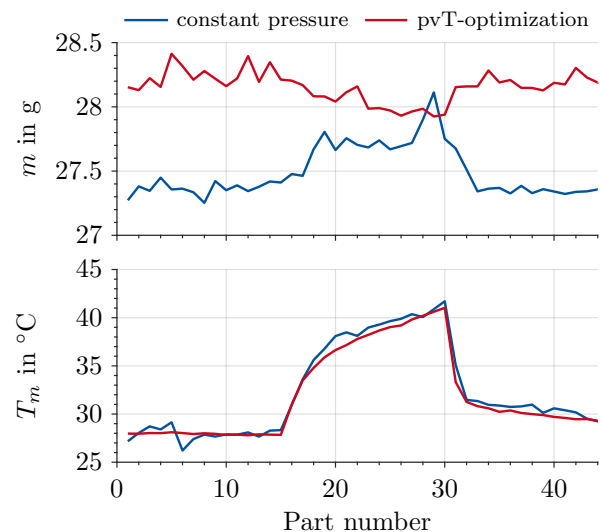


Fig. 7. Comparison of part weight m for a constant cavity pressure $r = 300$ bar and pvT-optimized reference.

ACKNOWLEDGEMENTS

The presented research was funded by the Deutsche Forschungsgemeinschaft (DFG, German Research Foundation) under Germany's Excellence Strategy – EXC-2023 Internet of Production – 390621612. The authors thank Arburg GmbH & Co. KG, Loßburg, Germany, and Sabic Deutschland GmbH & Co. KG, Dusseldorf, Germany, who provided machines and materials.

REFERENCES

- Agrawal, A.R., Pandelidis, I.O., and Pecht, M. (1987). Injection-molding process control - a review. *Polymer Engineering & Science*, 27(18), 1345–1357. doi:10.1002/pen.760271802.
- Bongart, W. (1982). *Verbesserte Prozeßführung durch selbsteinstellende Regelungen*. Ph.D. thesis, RWTH Aachen University.
- Brecher, C. (ed.) (2017). *Integrative Production Technology: Theory and Applications*. Springer International Publishing and Springer, Cham, 1st ed. 2017 edition.
- Butcher, J.C. (2008). *Numerical methods for ordinary differential equations*. Wiley, Hoboken, N.J. doi:10.1002/9780470753767.
- Chen, J.H., Sheu, L.J., Chen, W.C., Chen, H.K., and Chen, C.T. (2008a). Application of advanced process control in plastic injection molding. In *2008 IEEE International Conference on Service Operations and Logistics, and Informatics (SOLI)*, 2719–2724. doi:10.1109/SOLI.2008.4682997.
- Chen, W.C., Tai, P.H., Wang, M.W., Deng, W.J., and Chen, C.T. (2008b). A neural network-based approach for dynamic quality prediction in a plastic injection molding process. *Expert Systems with Applications*, 35(3), 843–849. doi:10.1016/j.eswa.2007.07.037.
- Djurdjanovic, D., Mears, L., Niaki, F.A., Haq, A.U., and Li, L. (2018). State of the art review on process, system, and operations control in modern manufacturing. *Journal of Manufacturing Science and Engineering*, 140(6). doi:10.1115/1.4038074.
- Dubay, R., Hu, B., Hernandez, J.M., and Charest, M. (2014). Controlling process parameters during plastication in plastic injection molding using model predictive control. *Advances in Polymer Technology*, 33(S1). doi:10.1002/adv.21449.
- Ferreau, H.J., Kirches, C., Potschka, A., Bock, H.G., and Diehl, M. (2014). qpOASES: A parametric active-set algorithm for quadratic programming. *Mathematical Programming Computation*, 6(4), 327 – 363. doi:10.1007/s12532-014-0071-1.
- Froehlich, C., Kemmetmuller, W., and Kugi, A. (2019). Model-predictive control of servo-pump driven injection molding machines. *IEEE Transactions on Control Systems Technology*, 1–16. doi:10.1109/tcst.2019.2918993.
- Gao, F., Patterson, W.I., and Kamal, M.R. (1994). Self-tuning cavity pressure control of injection molding filling. *Advances in Polymer Technology*, 13(2), 111–120. doi:10.1002/adv.1994.060130202.
- Grewal, M.S. and Andrews, A.P. (2008). *Kalman Filtering: Theory and Practice using Matlab*. John Wiley & Sons. doi:10.1002/9780470377819.
- Hakvoort, W., Aarts, R., van Dijk, J., and Jonker, J. (2007). Model-based iterative learning control applied to an industrial robot with elasticity. In *2007 46th IEEE Conference on Decision and Control*. IEEE. doi:10.1109/cdc.2007.4434366.
- Hopmann, C., Abel, D., Heinisch, J., and Stemmler, S. (2017). Self-optimizing injection molding based on iterative learning cavity pressure control. *Production Engineering*, 11(2), 97–106. doi:10.1007/s11740-017-0719-6.
- Hopmann, C., Reßmann, A., and Heinisch, J. (2016). Influence on product quality by pvt-optimised processing in injection compression molding. *International Polymer Processing*, 31(2), 156–165. doi:10.3139/217.3058.
- Kazmer, D. and Barkan, P. (1997). Multi-cavity pressure control in the filling and packing stages of the injection molding process. *Polymer Engineering & Science*, 37(11), 1865–1879. doi:10.1002/pen.11837.
- Li, C., Wang, F., Niu, D., and Liu, Y. (2010). Cavity pressure control by iterative learning control with zero-phase filtering in injection molding. In *2010 Chinese Control and Decision Conference (CCDC)*, 376–379. doi:10.1109/CCDC.2010.5499047.
- Lindert, S.O., Reindl, G., and Schlacher, K. (2014). Identification and control of an injection moulding machine. *IFAC Proceedings Volumes*, 47(3), 5878–5883. doi:10.3182/20140824-6-ZA-1003.01488.
- Michaeli, W. and Schreiber, A. (2009). Online control of the injection molding process based on process variables. *Advances in Polymer Technology*, 28(2), 65–76. doi:10.1002/adv.20153.
- Quarteroni, A., Sacco, R., and Saleri, F. (2007). *Numerical mathematics: With 45 tables*, volume 37 of *Texts in applied mathematics*. Springer, Berlin, 2. ed. edition. doi:10.1007/b98885.
- Reiter, M., Stemmler, S., Hopmann, C., Reßmann, A., and Abel, D. (2014). Model predictive control of cavity pressure in an injection moulding process. *IFAC Proceedings Volumes*, 47(3), 4358 – 4363. doi:10.3182/20140824-6-ZA-1003.02505.
- Schiffers, R. (2009). *Verbesserung der Prozessfähigkeit beim Spritzgießen durch Nutzung von Prozessdaten und eine neuartige Schneckenhubführung*. Ph.D. thesis, Universität Duisburg-Essen.
- Schmidt, T.W. (1986). *Zur Abschätzung der Schwindung*. Ph.D. thesis, RWTH Aachen University.
- Stemmler, S., Ay, M., Vukovic, M., Abel, D., Heinisch, J., and Hopmann, C. (2019). Cross-phase model-based predictive cavity pressure control in injection molding. *Proceedings of 3rd IEEE Conference on Control Technology and Applications (CCTA 2019)*.
- Tellaëche, A. and Arana, R. (2013). Machine learning algorithms for quality control in plastic molding industry. In *2013 IEEE 18th Conference on Emerging Technologies & Factory Automation (ETF A)*, 1–4. doi:10.1109/ETF A.2013.6648103.
- Thombansen, U., Buchholz, G., Frank, D., Heinisch, J., Kemper, M., Pullen, T., Reimer, V., Rotshteyn, G., Schwenzer, M., Stemmler, S., Abel, D., Gries, T., Hopmann, C., Klocke, F., Poprawe, R., Reisgen, U., and Schmitt, R. (2018). Design framework for model-based self-optimizing manufacturing systems. *The International Journal of Advanced Manufacturing Technology*, 97(1), 519–528. doi:10.1007/s00170-018-1951-8.